Díaz-Álvarez, A., Jiao-Wang, L., Feng, C. & Santiuste, C. (2020). Energy absorption and residual bending behavior of biocomposites bumper beams. *Composite Structures, 245*, 112343.

DOI: 10.1016/j.compstruct.2020.112343

ENERGY ABSORPTION AND RESIDUAL BENDING BEHAVIOUR OF BIOCOMPOSITES BUMPER BEAMS

Dedicated to our friend Prof. José Fernández-Sáez who passed away on March 31, 2020.

*A. Díaz-Álvarez[1], L. Jiao Wang[2], C. Feng[3], C. Santiuste[2]**

1 Department of Mechanical Engineering, University Carlos III of Madrid, Avda de la Universidad 30, 28911, Leganés, Madrid, Spain

2 Department of Continuum Mechanics and Structural Analysis, Universidad Carlos III de Madrid, Avda de la Universidad 30, 28911, Leganés, Spain

3 School of Civil Engineering, Nanjing Tech University, Nanjing, 211816 China

*Corresponding author: csantius@ing.uc3m.es

Abstract

This paper presents and analyzes the behavior of bumper beams made of PLA/flax composites subjected to low velocity impacts. The relevance of this material resides in the biodegradability of both fibers and matrix. Moreover, the after-impact behavior of this composite is excellent due to the absence of delamination. Impact tests have been performed using a drop weight tower within the range of impact energies 5 J $\leqslant E_{imp} \leqslant$ 73 J. The experimental setup enabled the measuring of impact velocity, residual velocity, load-time history and failure mode. Results show that damage generated during impact produces a significant reduction of residual stiffness but the residual strength is not affected by damage generated in the range of the applied impact energies considered.

Keywords: Biocomposite; Bumper; Energy Absorption; Natural fibers

1. INTRODUCTION

With the increase of motor vehicles worldwide, accidents have also been significantly increased, being frontal impacts the most likely to happen in the event of a collision [1]. In frontal accidents, the bumper is the first element of protection for passengers [2]. Thus, it is expected that it will be deformed enough to absorb the impact energy while maintaining its residual strength and stiffness to protect the critical components of the vehicle. Impact resistance is one of the most careful topics in the automotive industry [3,4]. In addition to the need to increase the bumpers

energy absorption capacity, it is also important for the saving of environmental footprint and the reduction of the vehicle weight [5].

Currently, most of the studies that can be found in the literature on bumpers are focused on optimizing the designs and manufacturing processes or on the use of new composites. In relation to the optimization of traditional bumpers, the main goal is the optimization of the section and thickness of the component [6,7]. Tanlak et al. [8] optimized the shape of a bumper beam to maximize its crashworthiness under impact conditions very similar to EuroNCAP tests. The results showed that the optimal beam shape presents a significant improvement over the one currently in-use; the specific absorbed energy is improved by 16% and the resistance to crash at low speeds is also significantly improved. Rao et al. [9] analyzed the crashworthiness of bumpers made with different materials and thicknesses. The results showed that the materials having high yield strength are best suited for the manufacturing of bumper beams; likewise, increasing the bumper beam thickness increases the rigidity and the impact resistance generated in the collision. Lee et al. [10] investigated cracks, defective forming, an improvement of the roll forming process for Aluminum 7075-T6 automotive bumper beam using GISSMO Damage. The results showed that the damage simulation due to GISSMO model was properly implemented including the influence of triaxiality and equivalent plastic strain of each bending part.

To improve fuel efficiency, many researchers try to replace metallic materials of the vehicle components with fiber reinforced plastic composites (FRP). The use of composites in the automotive industry is increasing exponentially thanks to their high specific strength, high specific stiffness and high energy absorption capability [11,12]. Within composites stand out for their growing use in the automotive structural parts the glass fiber reinforced plastics (GFRPs) and the carbon fiber reinforced plastics (CFRPs) [13]. Kim et al. [14] devised several designs of glass/carbon mat thermoplastic (GCMT) and their mechanical properties were calculated. The results showed that the optimally designed GCMT bumper beam had 33% less weight compared to the conventional glass mat thermoplastic (GMT bumper beam); moreover, the impact performance was improved. Davoodi et al. [15] studied a composite bumper beam as a reversible energy absorber with minimum parts under quasi-static compression. The results showed that the absorbed energy of composite bumper beam is enough for pedestrian impact and could be a real alternative to other materials such as expanded polypropylene (EPP).

In the last few years, 100% biodegradable composites, manufactured from natural fibers and matrices arise due to the growing environment concern and the need of materials with a low environmental footprint. In the automotive industry, biodegradable composites are used in several applications to limit the use of synthetic materials [16–18]. For instance, due to their lightness and low cost agave fibers are currently used in the automotive sector [19]. In addition, in some cases the manufacturing of biocomposites includes the use of materials from waste of different processes, like the lignin discarded in the manufacture of paper [20], and some others from farms [21].

However, although natural matrices can be used to obtain 100% biodegradable materials, natural fibers are typically used in conjunction with synthetic matrices (such as epoxy, polyethylene and polypropylene) to create hybrid composites [22,23]. Yan et al. [24] investigates the crashworthiness characteristics of natural flax fabric reinforced epoxy composite tubes as

an energy absorber. The results showed that the flax/epoxy tube is superior to conventional metal energy absorbers and close to that of glass/carbon fiber reinforced polymer composites. Aljibori et al. [25] studied experimentally the effect of geometry on crushing behaviour, energy absorption and failure mode of woven roving jute fiber/epoxy laminated composite tubes. The results showed that crashworthiness performance of jute composite depends on the geometry of the specimen. The circular jute composite tubes presented the highest energy absorption capacity.

Davoodi et al [26] focused on the mechanical properties of a hybrid kenaf/glass epoxy composite for utilization in a passenger car bumper beam. The results showed some advantages in comparison with the common bumper beam material glass mat thermoplastic (GMT). However, the impact performance is lower than the desirable level, which implies that the design of hybrid kenaf/glass bumper beams must be improved to be used in automotive industry. Faraj et al [27] determined the effect of supporting plates inside kenaf reinforced hexagonal tubes with variable side hexagonal angles in terms of the improvement of crashworthiness. The results showed that the use of supporting plates can improve the energy absorption capability up to 69% for all types of tested tubes. Ismail et al. [28] analyzed the crushing response of composite tubes fabricated with woven kenaf mats in different orientations and 2 or 3 layers. The analysis of the force-displacement curves showed that the best configurations were $[0^0/0^0]$ and $[0^0/0^0/0^0]$.

Although there are researches studying bumpers reinforced with natural fibers, and 100% biodegradable materials have been implemented in the automotive industry in several components [12,29,30], there are no studies analyzing bumper beams made of 100% natural composites (fiber and matrix). Previous works have shown the advantages of 100% biodegradable composites, manufactured from PLA and flax fibers, in terms of energy absorption capability and residual properties of flat square plates in comparison with CFRP plates [31-33].

Moreover, there is lack of knowledge concerning the residual strength of composite bumpers. The main goal of a bumper beam is the energy absorption capability in case of impact but the residual properties of the bumper are also important to be used in automotive industry. The after impact residual properties of composites laminates have received considerable attention in scientific literature, see for example the works of Ismail et al. [34] and Tuo et al. [35] for compression after impact (CAI) behavior and Santiuste et al. [36] for bending after impact properties (BAI). However, the after impact behavior of composite bumper beams is an almost unexplored field.

This work presents the first study of a bumper beam manufacture from 100% biodegradable composites. Bumper beam specimens made of flax/PLA composite were subjected to impact tests to analyze their energy absorption capability and damage mechanisms. The residual properties of impacted specimens were evaluated in three-point bending tests to estimate their residual bending strength and stiffness.

2. EXPERIMENTAL SETUP

2.1. Manufacturing

Flax/PLA bumper beams were manufactured using compression molding method, Fig. 1. Basket weave flax were used as reinforcement because it is one of the oldest crops in the world [37] and is widely used in the composite industry. Basket weave flax with 463.3 g/m^2 areal density, 0.94 mm of thickness and no chemical pre-treatment were cut into 300 mm x 300 mm plies.

PLA thermoplastic resin (10361D) provided by Nature Works LLC in pellets shape was used as matrix. The 10361D PLA is specifically aimed as a binder for the manufacture of biocomposites, its density is 1.24 g/cm^3 and melting temperature is around 145-170°C.

In the compression molding method pressure and temperature are applied by means of two thermo-heated plates in a universal testing machine. First, PLA films are obtained applying 4 MPa during 3 minutes at 185°C (pellets were previously kept in an oven at 95°C for 30 minutes to remove humidity). Then, a preheating 2 minutes without pressure at 185°C is applied to PLA films alternately stacked with woven flax plies. After preheating, a pressure of 16 MPa is applied for 3 minutes. At the end, the biocomposites panels were cooled between aluminum blocks in U shape (300x150x105 mm^3) that give the final bumper shape, Fig. 2*a*. All the parameters of the manufacturing process were optimized to improve the biocomposite mechanical properties in a previous work [38].

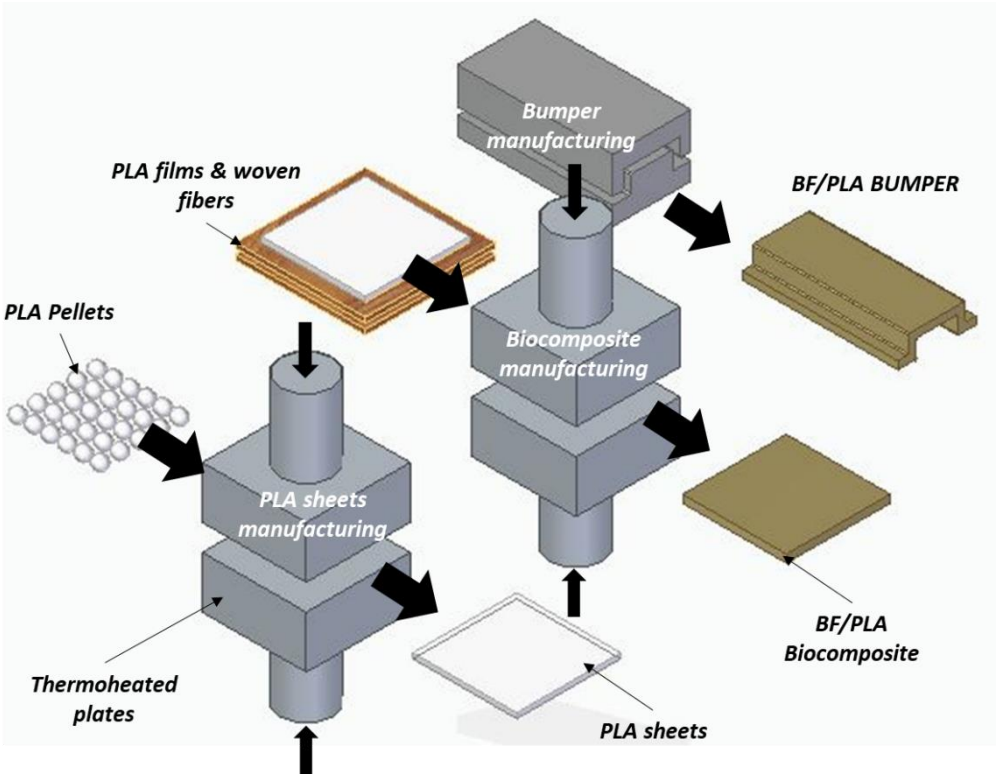

Figure 1. Bumper biocomposite manufacture route through compression molding method

2.2. Impact Tests

Low-velocity impact tests have been carried out in an INSTRON-CEAST Fractovist 6785 drop-weight tower. The specimens were hit orthogonally with an impactor bar which is free fall accelerated through a guide. The impactor nose had a Charpy shape with a diameter of 20 mm and a width of 65 mm. The impactor bar was instrumented to record the contact force during the impact. After the impact, an anti-rebound system held the impactor to avoid multi hits on the specimen. Impactor mass was fixed at 5.93 Kg while impact height ranged from 85.95 mm to 1275 mm. The minimum impact energy, 5 J, was selected because it produced a barely visible damage. While maximum impact energy, 73 J, produced serious damage including matrix cracking and fiber breakage. Eight impact energies were selected to analyze the influence of generated damage on the residual strength and stiffness of the specimens. For each impact energy three specimens were impacted allowing a check on repeatability. The specimens were placed on a steel plate and clamped at four point as can be seen in Fig. 2b. The experimental setup enabled the measuring of impact velocity, residual velocity and load-time history.

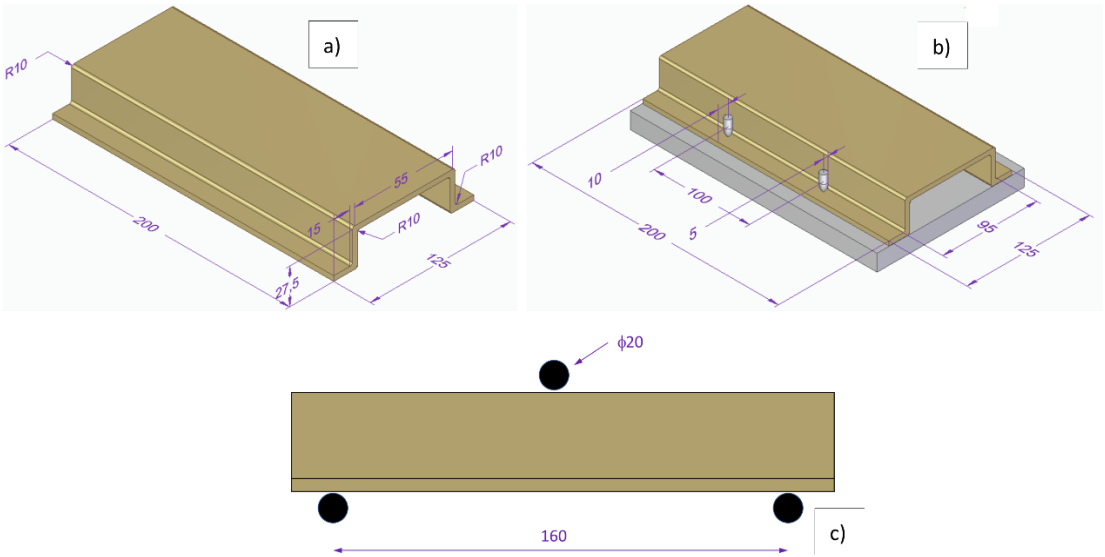

Figure 2. a) Scheme of the biocomposite bumpers; b) impact test configuration; c) Three-point bending test configuration. (dimensions in mm)

2.3. Bending After Impact (BAI)

Bending after impact tests were conducted to evaluate the residual properties of the impacted specimens in an Instron 8500 universal testing machine. Three-point bending configuration was selected according to the scheme shown in Fig. 2c. The specimen in BAI device is supported by two cylinders with a diameter of 20 mm to avoid stress concentration and a spam of 160 mm. The load was exerted with other cylinder with the same diameter in the middle cross section, thus maximum bending moment is applied at the impacted area. The velocity was fixed during the tests at 0.5 mm/min to avoid inertia force and consider quasi-static conditions. Load and displacement were recorded during tests.

3. IMPACT TESTS RESULTS

Fig. 3 shows the force displacement curves for different impact energies. These curves can be classified into two different groups. In the first group, for impact energies from 5 J to 30 J, force increases with displacement until the value of peak force is reached, then force and displacement decrease to zero. In the second group, from 40 J to 73 J, displacement continues increasing after the peak force is reached. The first group showed up an abrupt decrease in force once the peak force is reached. On the contrary, in the second group, it can be observed that force decreases to a plateau in which the force it is almost constant or in slight descent, until a drastically decrease at maximum displacement.

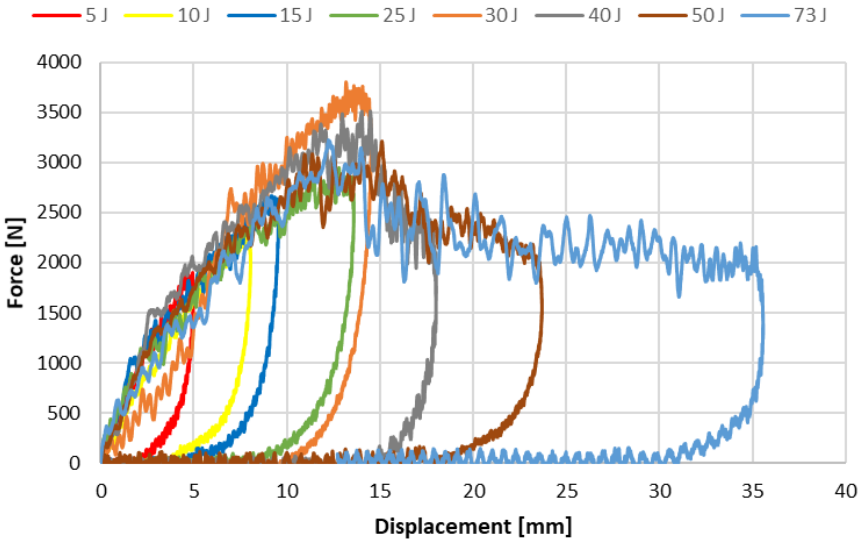

Figure 3. Peak load vs Displacement in Impact test of biocomposite bumpers.

Nevertheless, a general trend is observed for all impact energies, according to which, by increasing the impact energy, both peak force and maximum displacement increase. This trend agrees with those obtained by other authors for different composites [14,15,39]. Fig. 4 shows the maximum value of the contact force as a function of impact energy. For impact energies from 5 J to 30 J, peak force increases from 1927 N to 3753 N showing a practically linear trend. However, for impact energies from 30 J to 73 J, the value of peak force is almost constant around 3500 N. This indicates that fiber failure onset appears with a contact force of about 3500 N. This trend is consistent with that obtained by other authors for other composites [40,41]. The peak load is an important parameter that must be controlled, due to its influence in the risk for the vehicle occupants during the development of a vehicle frontal crash, being the lower peak load yields to lower decelerations and vice versa [4]. Present results indicate that peak load can be easily limited with natural fibers reinforced bumpers.

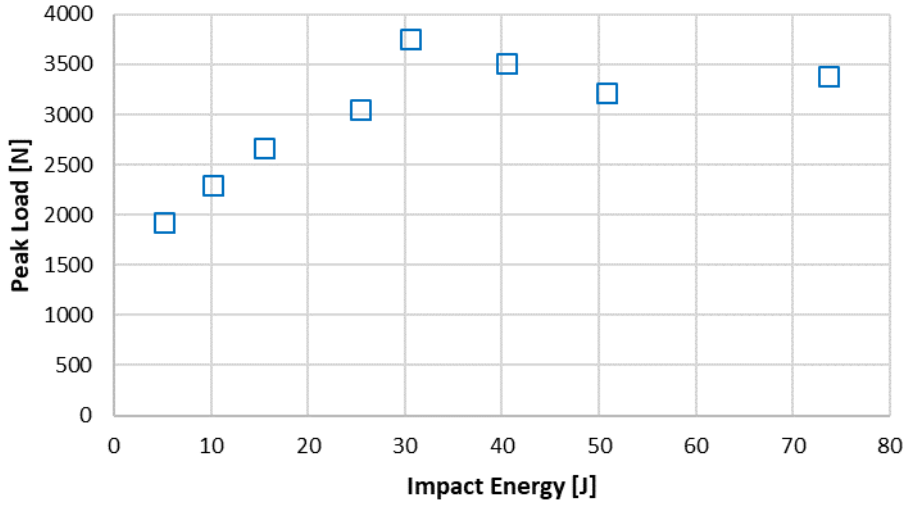

Figure 4. Peak Load vs Impact Energy for biocomposite bumpers.

During the impact tests similar damage mechanisms have been observed, mainly fiber breakage and matrix cracking in the impact area, not being detected delamination. Fig. 5 shows some impacted specimens for impact energies from 5 to 73 J. For lowest impact energy, 5J, only matrix cracking was found on the contact surface between impactor nose and bumper, Fig. 5a. For an impact energy of 25 J, matrix cracking was observed also in the borders between webs and top flange, Fig. 5b. Fiber breakage was detected in the borders between webs and top flange, if impact energy is 30 J or higher. In spite of the almost uniform value of the peak force from 30 to 73 J, the induced damage increases severely as can be observed comparing Figs. 5c-d.

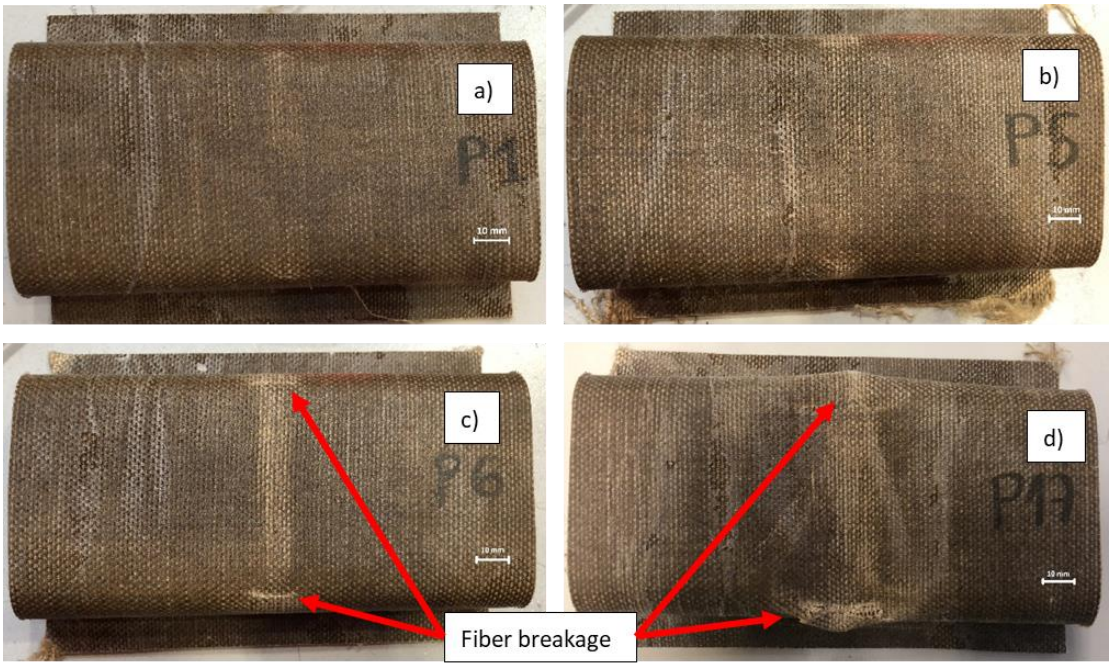

Figure 5. Biocomposite Bumpers after impact tests, top view of: a) E_{imp}= 5 J; b) E_{imp}= 25 J; c) E_{imp}= 30 J; d) E_{imp}= 73 J.

Fig. 6 shows representative curves of absorbed energy versus time. The curves follow the well-known trend in low-velocity impacts [34,42]. During the first stage, absorbed energy increases up to the value of impact energy. At this point, all the kinetic energy is absorbed by the bumper and the impactor velocity is zero. Then, the absorbed energy decreases while impactor is bouncing back and, finally, the value of absorbed energy is constant after the separation of bumper and impactor. The difference between the absorbed energy and the impact energy is the stored elastic energy that is converted again in the kinetic energy transferred to the impactor.

Two variables are influenced by the impact energy. The first one is that, obviously, absorbed energy increases with impact energy. The second effect is that the conversion of stored elastic energy into kinetic energy decreases with impact energy. This phenomenon can be clearly observed in Fig. 7, where the percentage of absorbed energy is plotted as a function of impact energy. The percentage of absorbed energy increases with impact energy from 79.29% for the lowest impact energy, 5 J, to 99.34% for the highest impact energy, 73 J. A low percentage of impact energy means that the impactor bounces back after the impact with the residual kinetic energy. While a percentage near 100% implies that the impactor is embedded on the bumper after the impact.

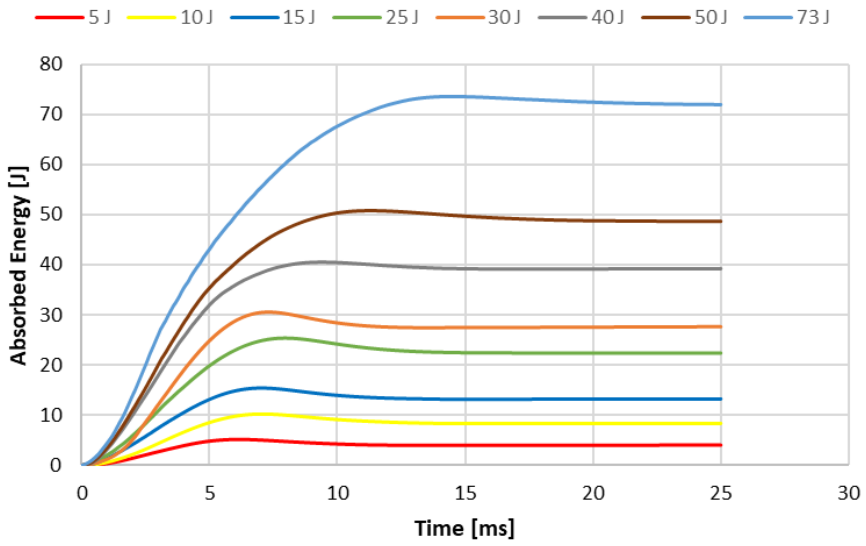

Figure 6. Absorbed energy vs time for flax bumpers impacted at different impact energies.

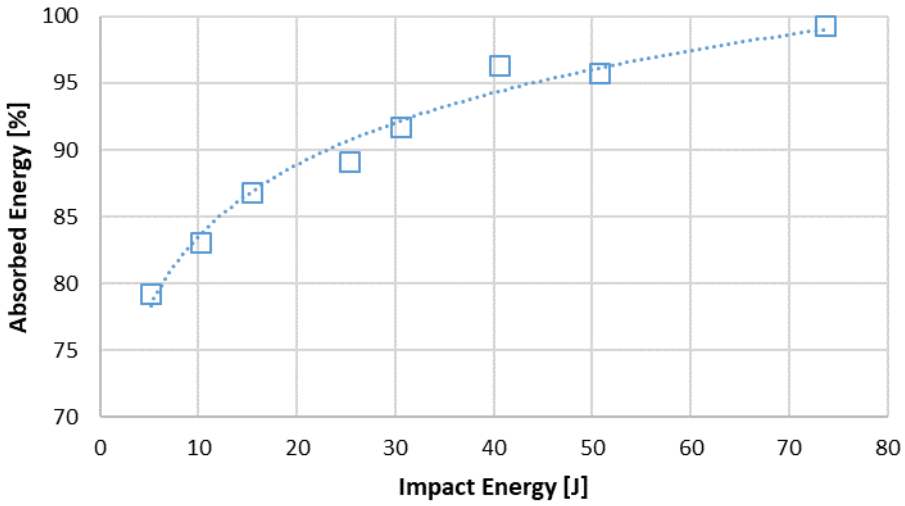

Figure 7. Percentage of Absorbed energy vs Impact energy for flax biocomposite bumpers.

4. BENDING AFTER IMPACT TESTS

Residual bending strength and stiffness of the impacted specimens have been quantified by means of three-point bending tests under static conditions. Non-impacted specimens have also been tested to be used as a reference.

Fig. 8 shows the force-displacement curves obtained in the bending after impact experimental tests for the biocomposite bumpers impacted at different energy levels. A comparison of these

force-displacement curves does not provide a clear tendency, thus peak force is plotted as a function of impact energy in Fig. 9 to analyze the influence of damage on the residual strength. The maximum values of peak load correspond to intermediate values of impact energy, 1668 N for 25 J and 1666 N for 30 J. On the other hand, the minimum value of peak force also corresponds to an intermediate impact energy, 1177 N for 40 J. These results indicate that residual strength is independent of damage generated during impact, probably because fiber failures produced in impact tests were oriented in perpendicular direction to the cross section, thus the fibers oriented in longitudinal direction are barely damage by the impacts. This trend is different to those reported by other authors in compressive after impact tests on composites laminates reinforced with glass/Flax fibres [34] or carbon fibers [35]. The reason of this discrepancy is attributed to the great influence of generated damage on bucking behavior, but the influence of this damage on the bending behavior is not so clear.

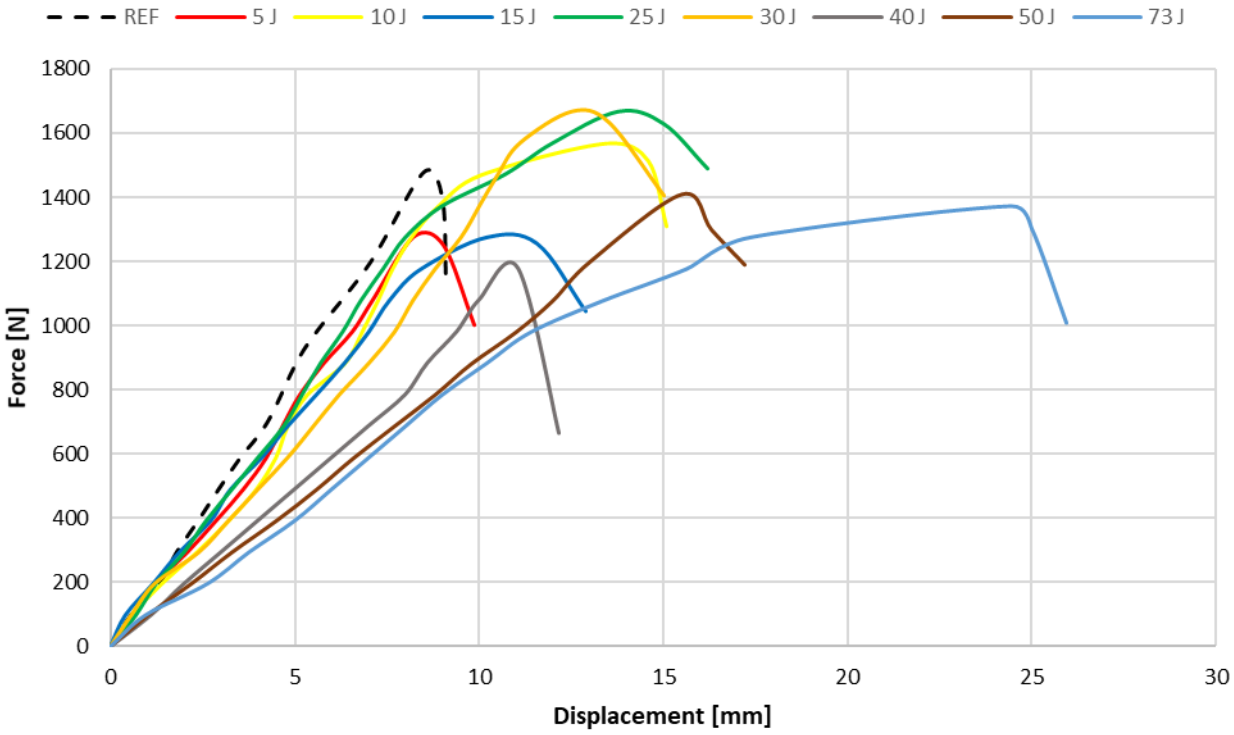

Figure 8. Force-Displacement graph for the bending after impact tests on biocomposite bumpers.

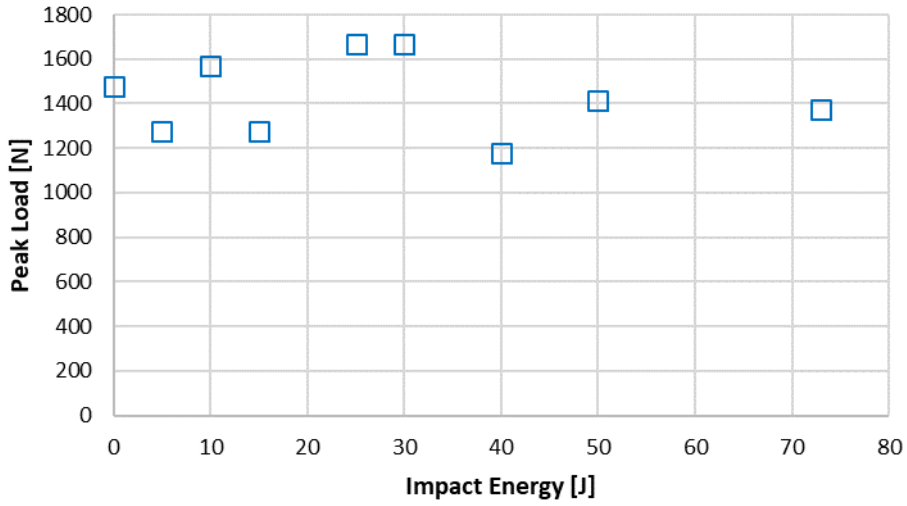

Figure 9. Peak load vs Impact Energy for bending after impact tests on biocomposites bumpers.

To analyses the influence of damage on the residual stiffness of the biocomposite bumpers, Fig. 10 shows the slope of the force-displacement curves as a function of impact energy. The minimum value of the slope, 85.93 N/mm, was obtained with the impact energy of 73 J, while the maximum value of the slope, 169,96 N/mm, was obtained in the unimpacted specimen. The slope of the force-displacement curve is almost constant, around 160 N/mm for impact energy lower than 30 J. However, for impact energies higher or equal to 30 J the slope of force-displacement curves decreases with impact energy. Thus, the stiffness of the bumper is not significantly affected by the impact when the main failure mechanism is matrix cracking as was observed for impact energies lower than 30 J. However, when fiber failure is produced during impact, as was observed for impact energies higher than 30 J, the bumper stiffness is drastically reduced.

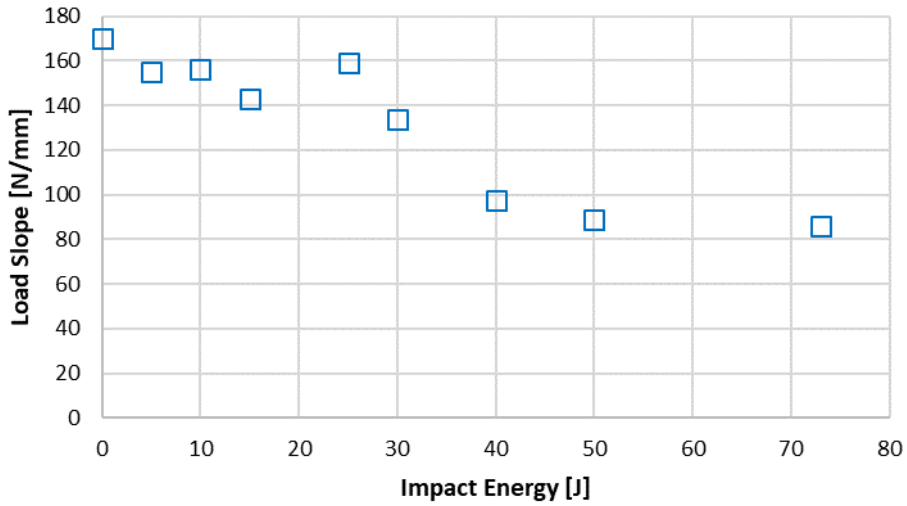

Figure 10. Peak Load Slope vs Impact Energy for bending after impact tests on biocomposite bumpers.

5. CONCLUSIONS

This paper analyses the impact and post-impact behavior of fully biodegradable composites bumper beams subjected to low-velocity impact. A drop weight tower has been used to perform impact tests at different impact energies in the range 5 J $\leqslant E_{imp} \leqslant$ 73 J, from barely visible damage to serious damage including matrix cracking and fiber breakage. Residual bending strength and stiffness were estimated through three-point bending tests to evaluate the effect of damage on post-impact behavior of bumper beams. The following main conclusions are drawn:

- If impact energy is between 5 J and 30 J, peak force increases with impact energy. But for impact energies from 30 J to 73 J, the value of peak force is almost constant around 3500 N. These two trends are related to different failure mechanisms observed in impacted specimens. For impact energies lower than 30 m, the main failure mechanism is matrix cracking, while fiber breakage appears for impact energies of 30 J or higher.
- The results of after impact bending tests show that, in the range of the applied impact energies considered, the induced damage during impact does not influence on residual strength. This unexpected result can be explained by the orientation of damage fibers, bending strength is dominated by fibers oriented in the longitudinal direction of the beam while broken fibers are oriented in perpendicular direction.
- The results of residual stiffness can be divided into two groups. For impact energies lower than 30 J, the residual stiffness is not affected by damage generated during impact because the main failure mechanism is matrix cracking. However, for impact energies higher or equal to 30 J, the residual stiffness decreases with impact energy. Delamination was not observed in any specimen.

In forthcoming studies, it would be necessary to make progress in the analysis of the failure mechanisms to explain why fiber failure generated when impact energy is higher than 30 J reduces residual stiffness but residual strength is unaffected. Moreover, a study considering different impactor nose shape is necessary to modify the distribution of generated damage.

ACNOWLEDGMENTS

Authors gratefully acknowledges the support of Spanish Ministry of Economy under the project DPI2013-43994-R.

REFERENCES

[1] ChanWorld Health Organization. (2015). Global status report on road safety 2015. World Health Organization.

[2] Wang C, Wang W, Zhao W, Wang Y, Zhou G. Structure design and multi-objective optimization of a novel NPR bumper system. Compos Part B 2018;153:78–96.

doi:10.1016/j.compositesb.2018.07.024.

[3] Liu Z, Lu J, Zhu P. Lightweight design of automotive composite bumper system using modified particle swarm optimizer. Compos Struct 2016;140:630–43. doi:10.1016/j.compstruct.2015.12.031.

[4] Belingardi G, Beyene AT, Koricho EG, Martorana B. Alternative lightweight materials and component manufacturing technologies for vehicle frontal bumper beam. Compos Struct 2015;120:483–95. doi:10.1016/j.compstruct.2014.10.007.

[5] Merklein M, Geiger M. New materials and production technologies for innovative lightweight constructions 2002;126:532–6.

[6] Qian L, Paredes M, Wierzbicki T, Sparrer Y, Feuerstein M. Experimental and numerical study on shear-punch test of 6060 T6 extruded aluminum profile. Int J Mech Sci 2016;118:205–18. doi:10.1016/j.ijmecsci.2016.09.008.

[7] Sun G, Pang T, Fang J, Li G, Li Q. Parameterization of criss-cross configurations for multiobjective crashworthiness optimization. Int J Mech Sci 2017;124–125:145–57. doi:10.1016/j.ijmecsci.2017.02.027.

[8] Tanlak N, Sonmez FO, Senaltun M. Shape optimization of bumper beams under high-velocity impact loads. Eng Struct 2015;95:49–60. doi:10.1016/j.engstruct.2015.03.046.

[9] Rao DSS, Viswatej K, Adinarayana DS. Design and Sensitivities Analysis on Automotive Bumper Beam Subjected to Low Velocity Impact 2016;37:110–21.

[10] Lee S, Lee J, Song J, Park J, Choi S. Fracture simulation of cold roll forming process for aluminum automotive bumper beam using GISSMO damage model 7075-T6 automotive bumper beam using GISSMO damage model Costing models for capacity optimization in Industry Fracture simulation of cold roll f. Procedia Manuf 2018;15:751–8. doi:10.1016/j.promfg.2018.07.314.

[11] Safri A, Thariq M, Sultan H, Jawaid M. Impact behaviour of hybrid composites for structural applications : A review 2018;133:112–21. doi:10.1016/j.compositesb.2017.09.008.

[12] Koronis G, Silva A, Fontul M. Composites : Part B Green composites : A review of adequate materials for automotive applications. Compos Part B 2013;44:120–7. doi:10.1016/j.compositesb.2012.07.004.

[13] Badie MA, Mahdi E, Hamouda AMS. An investigation into hybrid carbon / glass fiber reinforced epoxy composite automotive drive shaft. Mater Des 2011;32:1485–500. doi:10.1016/j.matdes.2010.08.042.

[14] Kim D, Kim H, Kim H. Design optimization and manufacture of hybrid glass / carbon fiber reinforced composite bumper beam for automobile vehicle. Compos Struct 2015;131:742–52. doi:10.1016/j.compstruct.2015.06.028.

[15] Davoodi MM, Sapuan SM, Yunus R. Materials & Design Conceptual design of a polymer composite automotive bumper energy absorber 2008;29:1447–52. doi:10.1016/j.matdes.2007.07.011.

[16] Díaz-álvarez A, Díaz-álvarez J, Santiuste C, Miguélez MH. Experimental and numerical analysis of the influence of drill point angle when drilling biocomposites. Compos Struct

2019;209:700–9. doi:10.1016/j.compstruct.2018.11.018.

[17] Omrani E, Menezes PL, Rohatgi PK. State of the art on tribological behavior of polymer matrix composites reinforced with natural fibers in the green materials world. Eng Sci Technol an Int J 2016;19:717–36. doi:10.1016/j.jestch.2015.10.007.

[18] Li Y, Mai YW, Ye L. Sisal fibre and its composites: a review of recent developments. Compos Sci Technol 2000;60:2037–55. doi:10.1016/S0266-3538(00)00101-9.

[19] Mancino A, Marannano G, Zuccarello B, Mancino A. Implementation of eco-sustainable biocomposite materials reinforced by optimized agave fibers reinforced by optimized agave fibers modeling of a high a pressure turbine a blade of an airplan 2018;00. doi:10.1016/j.prostr.2017.12.052.

[20] Yamini G, Shakeri A, Zohuriaan-mehr MJ, Kabiri K. Cyclocarbonated lignosulfonate as a bio-resourced reactive reinforcing agent for epoxy biocomposite : From natural waste to value-added bio- additive. J CO2 Util 2018;24:50–8. doi:10.1016/j.jcou.2017.12.007.

[21] Yzombard A, Gordon SG, Miao M. Morphology and tensile properties of bast fibers extracted from cotton stalks. Text Res J 2013;84:303–11. doi:10.1177/0040517513495949.

[22] Arbelaiz A, Fernández B, Cantero G, Llano-Ponte R, Valea A, Mondragon I. Mechanical properties of flax fibre/polypropylene composites. Influence of fibre/matrix modification and glass fibre hybridization. Compos Part A Appl Sci Manuf 2005;36:1637–44. doi:10.1016/j.compositesa.2005.03.021.

[23] Díaz-Álvarez A, Rubio-López Á, Santiuste C, Miguélez MH. Experimental analysis of drilling induced damage in biocomposites. Text Res J 2018;88:2544–58. doi:10.1177/0040517517725118.

[24] Yan L, Chouw N. Crashworthiness characteristics of flax fibre reinforced epoxy tubes for energy absorption application. Mater Des 2013;51:629–40. doi:10.1016/j.matdes.2013.04.014.

[25] Aljibori HSS. Energy Systems and Crushing Behavior of Fiber Reinforced Composite Materials 2011;5:349–55.

[26] Davoodi MM, Sapuan SM, Ahmad D, Ali A, Khalina A, Jonoobi M. Mechanical properties of hybrid kenaf / glass reinforced epoxy composite for passenger car bumper beam. Mater Des 2020;31:4927–32. doi:10.1016/j.matdes.2010.05.021.

[27] Faraj M, Alkbir A, Sapuan M, Aziz A, Ishak MR. Lateral Crushing Properties of Non-Woven Kenaf (Mat) - Reinforced Epoxy Composite Hexagonal Tubes 2016;17:965–72. doi:10.1007/s12541-016-0118-5.

[28] Ismail AE. Kenaf Fiber Reinforced Composites Tubes as Energy Absorbing Structures 2016:2–6.

[29] Lau K, Hung P, Zhu M, Hui D. Properties of natural fi bre composites for structural engineering applications. Compos Part B 2018;136:222–33. doi:10.1016/j.compositesb.2017.10.038.

[30] Dittenber DB, Gangarao HVS. Critical review of recent publications on use of natural composites in infrastructure. Compos Part A Appl Sci Manuf 2012;43:1419–29.

doi:10.1016/j.compositesa.2011.11.019.

[31] Rubio-López A, Artero-Guerrero J, Pernas-Sánchez J, Santiuste C. Compression after impact of flax/PLA biodegradable composites. Polym Test 2017;59:127-135. doi:10.1016/j.polymertesting.2017.01.025

[32] Rubio-López A, Olmedo A, Santiuste C. Modelling impact behaviour of all-cellulose composite plates. Compos Struct 2015;122:139–43. doi:10.1016/j.compstruct.2014.11.072.

[33] Huber T, Bickerton S, Müssig J, Pang S, Staiger MP. Flexural and impact properties of all-cellulose composite laminates. Compos Sci Technol 2013;88:92–8. doi:10.1016/j.compscitech.2013.08.040.

[34] Ismail KI, Sultan MTH, Shah AUM, Jawaid M, Safri SNA. Low velocity impact and compression after impact properties of hybrid bio-composites modified with multi-walled carbon nanotubes. Compos Part B Eng 2019;163:455–63. doi:10.1016/j.compositesb.2019.01.026.

[35] Tuo H, Lu Z, Ma X, Zhang C, Chen S. An experimental and numerical investigation on low-velocity impact damage and compression-after-impact behavior of composite laminates. Compos Part B Eng 2019;167:329–41. doi:10.1016/j.compositesb.2018.12.043.

[36] Santiuste C, Sánchez-Sáez S, Barbero E. Residual flexural strength after low-velocity impact in glass/polyester composite beams. Compos Struct 2010;92:25–30. doi: 10.1016/j.compstruct.2009.06.007.

[37] Amiri A, Triplett Z, Moreira A, Brezinka N, Alcock M, Ulven CA. Standard density measurement method development for flax fiber. Ind Crops Prod 2017;96:196–202. doi:10.1016/j.indcrop.2016.11.060.

[38] Rubio-López A, Olmedo A, Díaz-Álvarez A, Santiuste C. Manufacture of compression moulded PLA based biocomposites: A parametric study. Compos Struct 2015;131:995–1000. doi:10.1016/j.compstruct.2015.06.066.

[39] Xiao Z, Fang J, Sun G, Li Q. Advances in Engineering Software Crashworthiness design for functionally graded foam-filled bumper beam. Adv Eng Softw 2015;85:81–95. doi:10.1016/j.advengsoft.2015.03.005.

[40] Mihael C, Ramona D, Laurentiu DC. The impact behaviour of composite materials. 3rd Int Conf Marit Nav Sci Eng 2010:45–50.

[41] G.A. Schoeppner. Delamination threshold loads for low velocity impact on composite laminates. Compos Part A Appl Sci Manuf 2000;31:903–15. doi:10.1016/S1359-835X(00)00061-0.

[42] Tita V, de Carvalho J, Vandepitte D. Failure analysis of low velocity impact on thin composite laminates: Experimental and numerical approaches. Compos Struct 2008;83:413–28. doi:10.1016/j.compstruct.2007.06.003.